Biomass and Bioenergy 173 (2023) 106781

Contents lists available at ScienceDirect

Biomass and Bioenergy

journal homepage: www.elsevier.com/locate/biombioe

Biogas reforming to syngas in a DBD plasma reactor with dielectric materials packing: Effect of H_2S on the conversion of CH_4 and CO_2

M. Umamaheswara Rao [a], Divakar Singh [b], KVSS Bhargavi [a], Ranjan Kumar Sahu [c], Saket Asthana [c], Ch. Subrahmanyam [a,*]

[a] Department of Chemistry, Indian Institute of Technology Hyderabad, Kandi, Sangareddy, Telangana, 502284, India
[b] Department of Climate Change, Indian Institute of Technology Hyderabad, Kandi, Sangareddy, Telangana, 502284, India
[c] Department of Physics, Indian Institute of Technology Hyderabad, Kandi, Sangareddy, Telangana, 502284, India

ARTICLE INFO

Keywords:
Biogas reforming
DBD plasma discharge
Syngas
Dielectric material

ABSTRACT

Biogas is a renewable energy produced due to the anaerobic decomposition of plants and animals. Biogas contains a high amount of methane (CH_4), carbon dioxide (CO_2), and trace amounts of hydrogen sulfide (H_2S). It is naturally released in the environment, and the composition varies depending on the source it is generated. The primary focus of the study is to understand the influence of H_2S on CH_4 and CO_2 conversion during syngas production. The effect of applied voltage on biogas reforming reaction with different dielectric materials (glass beads, γ-Al_2O_3, ZrO_2, and quartz wool) packed in a discharge zone was investigated by using a dielectric barrier discharge (DBD) non-thermal plasma reactor. The influence of gas composition and packed bed on the efficiency of the biogas reforming reaction was investigated. After that, the biogas reforming reaction with packed dielectric material was performed without H_2S and subsequently with H_2S (blended with N_2) while keeping the residence time constant. It was observed that H_2S has a significant effect on the conversion. The CH_4 conversion drastically dropped from 23% (without H_2S) to 9% (with H_2S), and CO_2 conversion dropped from 18% to 11 % at 22 kV with quartz wool packed DBD. Energy efficiency decreased from 3.12 mmol/kJ (without H_2S) to 1.78 mmol/kJ (with H_2S) with glass beads packed DBD. Moreover, H_2S has more effect on CH_4 conversion than CO_2.

1. Introduction

The world's fossil fuel consumption has been increasing over the years, and as a result, carbon dioxide (CO_2) concentration in the atmosphere is also increasing substantially [1]. Consequently, controlling CO_2 emissions is crucial for maintaining the ecosystem. The two potential greenhouse gases, CH_4 and CO_2, have many negative effects, including global warming [1]. Biogas is a renewable resource produced by the anaerobic digestion of raw materials such as agricultural waste, fertilizers, municipal waste, plant materials, sewage, and food waste. Human activities such as livestock farming, rice cultivation, and waste accumulation in large landfills release significant amounts of biogas, increasing CH_4 and CO_2 concentrations in the atmosphere [2]. Biogas composition is based on its source, mainly 35–75% CH_4, 25–50% CO_2, and traces of contaminants such as H_2S [3].

CH_4 can be transformed into heat and electricity using various processes like dry reforming, steam reforming, and partial oxidation of methane. Equations (i)-(iii) are the three basic strategies for converting CH_4 in biogas to H_2 and CO [4,5].

$$CH_4 + CO_2 \rightarrow 2CO + 2H_2 \Delta H = 247\ kJ/mol \quad (i)$$

$$CH_4 + H_2O \rightarrow CO + 3H_2 \Delta H = 206\ kJ/mol \quad (ii)$$

$$CH_4 + \frac{1}{2}O_2 \rightarrow CO + 2H_2 \Delta H = -36\ kJ \Big/ mol \quad (iii)$$

Biogas is a renewable energy source and has the potential to meet urban society's energy demand. Syngas is an important chemical feedstock for manufacturing liquid chemicals such as alcohols and hydrocarbons via the Fischer-Tropsch process [6,7]. On a close look, reforming biogas to syngas (CO and H_2) without CO_2 separation or capture is an economical approach for biogas utilization and energy production [8]. Furthermore, this technique can provide a renewable energy source with no carbon emission into the atmosphere [9–11]. However, commercial-scale thermo-catalytic biogas reforming is inefficient due to its high operating energy cost and highly endothermic

* Corresponding author.
E-mail address: csubbu@chy.iith.ac.in (Ch. Subrahmanyam).

https://doi.org/10.1016/j.biombioe.2023.106781
Received 29 September 2022; Received in revised form 25 February 2023; Accepted 27 March 2023
Available online 12 April 2023

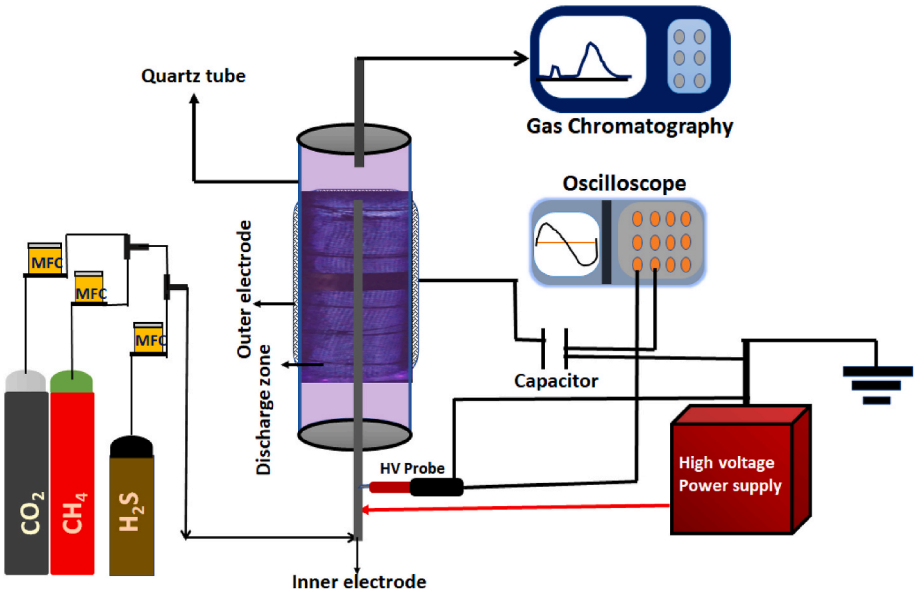

Fig. 1. Schematic diagram of the experimental set-up.

nature. Also, catalyst deactivation is caused by carbon deposition, particularly at high CH_4/CO_2 ratios [12].

Non-thermal plasma (NTP) has been identified as a promising alternative to traditional thermal catalytic processes for converting biogas to valuable fuels and chemicals at low temperatures and atmospheric pressure [13–16]. The primary advantage of NTP is its non-equilibrium property, resulting in mean electron energies between 1 and 10 eV while the background gas temperature remains at ambient conditions [17]. This electron energy range is optimal for exciting the molecular and atomic species and breaking chemical bonds through electron impact excitation, dissociation, and ionization [18,19]. However, combining a solid catalyst with non-thermal plasma leads to a synergy between plasma and catalyst [13,14,20,21]. The catalytic non-thermal plasma approach significantly improves the reactant conversion, selectivity, and yield of desired products and process energy efficiency. The transformation of biogas into value-added chemicals and fuels by plasma catalysis involves physical and chemical reactions.

Furthermore, plasma and catalyst have a synergistic effect on enhancing the selectivity and yield of the product molecules. However, the biogas reforming reaction in the plasma reactor may result in coke deposition on the catalyst's surface, reducing the catalytic activity. The reactor was packed with a dielectric material, and although carbon was produced during the reaction, it does not affect the material's performance. In addition, the presence of H_2S decreases the efficiency of the process. In this context, using dielectric materials can avoid synergistic effects and may withstand sulfur poisoning [14,22,23]. Various non-thermal plasma reactors have been applied for biogas reforming, including dielectric barrier discharge (DBD) reactor [24,25], corona discharge [26,27], glow discharge [28,29], gliding arc discharge [30–32]. DBD has grown in popularity for the low-temperature synthesis of fuels and chemicals due to its simple design and upscaling [33].

Yuxuan Zeng et al. (2022) studied the biogas reforming with Ni–K/Al_2O_3 packed in the DBD reactor to improve CO_2 and CH_4 conversion and obtained a syngas ratio of 2.7 at 340 °C [34]. Asencios et al. (2011) performed biogas reform using NiO/MgO/ZrO_2 in the presence of air and produced an H_2/CO ratio of 1.1 [35]. Xu et al. (2010) tested biogas reformation in a fixed bed reactor using an inlet gas of CH_4 and CO_2 (1:1) and obtained a syngas ratio of 0.9 at 800 °C [36]. Xin Tu et al. (2012) obtained a syngas gas ratio of 0.91 when the applied power was 50 W [16]. Even though several studies have been done on biogas reforming, most have focused on a model gas combination without H_2S. In this study, we explored the biogas reforming reaction, even in the presence of H_2S in a DBD reactor packed with dielectric materials such as glass beads, γ-Al_2O_3, ZrO_2, and quartz wool. The main objective of this study was to investigate the effect of H_2S on biogas reforming reaction. With the addition of H_2S, the poisoning effect on the feed gas composition was studied in terms of reduced CH_4 and CO_2 conversions and syngas ratio. The plasma with the dielectric material process was studied and initially with varying CH_4/CO_2 molar ratio and packed bed effect.

2. Experimental section

2.1. Experimental set-up

Fig. 1 shows the dielectric barrier discharge reactor used for biogas reforming. The flow rate was fixed at 70 mL min^{-1}. A quartz tube with an inner diameter of 18 mm with a stainless-steel mess wrapped around the quartz tube serves as a ground electrode. An inner electrode of 9 mm diameter placed at the center of the quartz tube serves as the high voltage electrode, and the resulting discharge gap was 4.5 mm. The discharge volume was 21 cm^3, and the residence time of gas was 18 s. A digital oscilloscope recorded the electrical signal (Rigol DS1104Z plus). The dissipated power was calculated by the Q-U Lissajous method. Initially, the reaction was performed with CO_2 (30 mL min^{-1}), CH_4 (30 mL min^{-1}), and N_2 (10 mL min^{-1}) through the DBD reactor without packing and packing with dielectric materials. After that, we added 10 mL of H_2S (0.054%) to a mixture of CH_4 and CO_2 while keeping the residence time constant.

2.2. Gas analysis and parameter definitions

Gaseous products were analyzed by gas chromatography (Mayura Analytical Pvt. Ltd.) equipped with a thermal conductivity detector. The products were eluted using Molecular Sieve 5A and HayaSep-A columns. The parameters were calculated from the following equations.

$$CH_4 \text{ conversion } (\%) = \frac{CH_4 \text{ converted (mmol/min)}}{CH_4 \text{ input (mmol/min)}} \times 100 \quad (1)$$

$$CO_2 \text{conversion } (\%) = \frac{CO_2 \text{ converted (mmol/min)}}{CO_2 \text{input (mmol/min)}} \times 100 \quad (2)$$

Table 1
Plasma parameters for biogas reforming in the absence of H_2S.

Packing material	Applied Voltage (kV)	Power (W)	C_d (μF)	Q pk-pk (μC)	dQ (μC)	U_b (kV)
No packing	22	1.8	2.0	11.6	10.0	5.0
Glass beads	22	2.1	2.2	12.5	11.1	4.8
γ-Al_2O_3	22	2.8	2.3	12.7	12.0	4.5
ZrO_2	22	2.9	2.3	12.8	12.3	4.8
Quartz wool	22	3.2	2.4	12.9	12.5	4.4

$$\text{CO selectivity } (\%) = \frac{\text{CO Produced (mmol/min)}}{[\text{CH}_4 \text{ converted} + \text{CO}_2 \text{ converted}](\text{mmol/min})} \times 100 \quad (3)$$

$$\text{H}_2 \text{ selectivity } (\%) = \frac{\text{H}_2\text{Produced (mmol/min)}}{2 \times \text{CH}_4 \text{ converted (mmol/min)}} \times 100 \quad (4)$$

$$\text{CO yield } (\%) = \frac{\text{CO Produced (mmol/min)}}{[\text{CH}_4 \text{ input} + \text{CO}_2 \text{ input}](\text{mmol/min})} \times 100 \quad (5)$$

$$\text{H}_2 \text{ yield } (\%) = \frac{\text{H}_2 \text{ Produced (mmol/min)}}{2 \times \text{CH}_4\text{input (mmol/min)}} \times 100 \quad (6)$$

$$\frac{\text{H}_2}{\text{CO}} = \frac{\text{H}_2\text{Produced (mmol/min)}}{\text{CO Produced (mmol/min)}} \quad (7)$$

$$\text{CB } (\%) = \frac{[\text{CH}_4 \text{ output} + \text{CO}_2 \text{ output}] + \text{CO produced (mmol/min)}}{[\text{CH}_4 \text{ input} + \text{CO}_2 \text{ input }](\text{mmol/min})} \times 100 \quad (8)$$

$$\text{Energyefficiency (mmol/kJ)} = \frac{[\text{CH}_4 \text{ converted} + \text{CO}_2 \text{ converted}](\text{mmol/min})}{\text{Power (W)}} \times \frac{1000}{60} \quad (9)$$

3. Results and discussion

3.1. Discharge characteristics with various dielectric-packed materials

Biogas reforming reaction carried out in a DBD non-thermal plasma reactor with dielectric materials such as glass beads, γ-Al_2O_3, ZrO_2 beads, and quartz wool. The discharge without packing, typically a filamentary discharge, was created in the discharge zone. When a dielectric material is packed into the whole discharge area, it creates a packed-bed effect. It changes the discharge from a filamentary discharge to a combination of a surface discharge and a filamentary discharge [37]. Therefore, it is possible for the charge to build up on the surface of the dielectric material. Because of this, the electric field strength and electron temperature have been enhanced. A DBD plasma with packing materials produces more electrons with high energy. Most of the energy is transferred to the various channels of excitation, ionization, and dissociation of CO_2 and CH_4 [38]. The dissipated power during the plasma discharge was calculated from the Lissajous method. The power was increased with applied voltage increases in all the cases. Several discharge parameters, such as dielectric capacitance, peak-to-peak charge transfer, charge transfer per half cycle, and breakdown voltage, were calculated from the Lissajous figure, which is shown in Fig. S1 and listed in Table 1. The discharge parameters significantly changed when we introduced dielectric materials into the DBD reactor compared to no packed DBD. Even though the parameters of the discharge do not vary much when different dielectric materials are used. Among all packed materials, quartz wool packed DBD has been increased micro discharges lead to high current pulses, producing highly energetic electrons during the discharge. From Fig. 2a it was observed that DBD packed with dielectric materials improved the electric field strength, so that power increased in all packed conditions compared to no packed DBD. Quartz wool packed DBD dissipated the highest power during the discharge. Therefore, quartz wool has the lowest breakdown voltage among the studied materials. When plasma ignites, gas breakdown occurs in the discharge-on phase, but the discharge-off phase develops when a displacement current is present in the circuit. Discharge characteristics are also affected in the biogas reforming reaction with the addition of H_2S. The power dissipation was significantly reduced with H_2S addition to the gas mixture due to the poison effect of H_2S, which is shown in Fig. 2b.

3.2. Effect of dielectric materials on biogas reforming

The packed materials dielectric constant was determined using an impedance analyzer (Wayne Kerr 6500 B). The experiment was carried out at room temperature and in the frequency range of 20 Hz-1MHz. The frequency-dependent dielectric constant plot data are shown in Figs. S2 and S3. The dielectric constant value of packed materials decreases with increasing frequency and approaches unity at higher frequencies. This result can be linked to the release of space charge polarization and dipolar polarization as frequency increases. The varying dielectric constant values of packed materials with frequency showed in Tables S2 and S3. Dielectric constant and shape of packing materials play a major role in the biogas reforming reaction. The best reaction performance was achieved with quartz wool packed DBD. Even though quartz wool has a dielectric constant of ~5, it is made up of fragile and flexible quartz fibers and displayed intense discharges when high voltage was applied. In glass beads, ZrO_2 beads, and γ-Al_2O_3 beads packed DBD reactor, the available space for the formation of discharge becomes limited in the discharge zone. Therefore, among all packed materials, quartz wool packed DBD exhibited better reaction efficiency. The packing material's electric field strength directly affects the discharge's physical

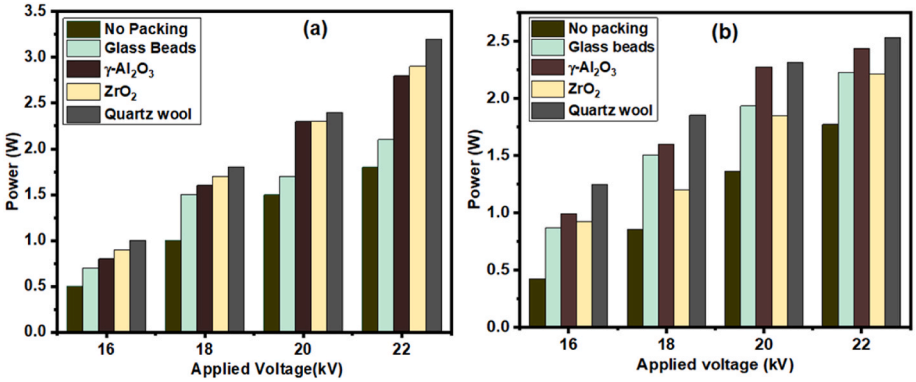

Fig. 2. Variation of Power with applied voltage (a) without H_2S and (b) with H_2S.

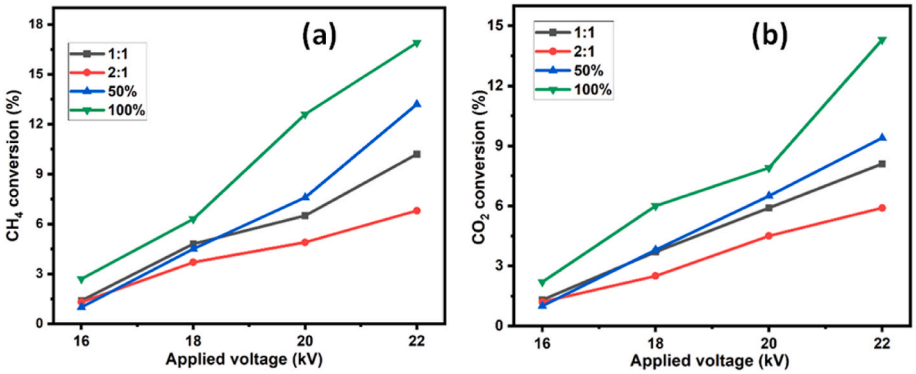

Fig. 3. (a) Represents the effect of feed gas ratio and packed bed effect on the CH_4 conversion (b) CO_2 conversion with applied voltage with a fixed flow rate of 70 mL min^{-1} and fixed frequency of 50 Hz.

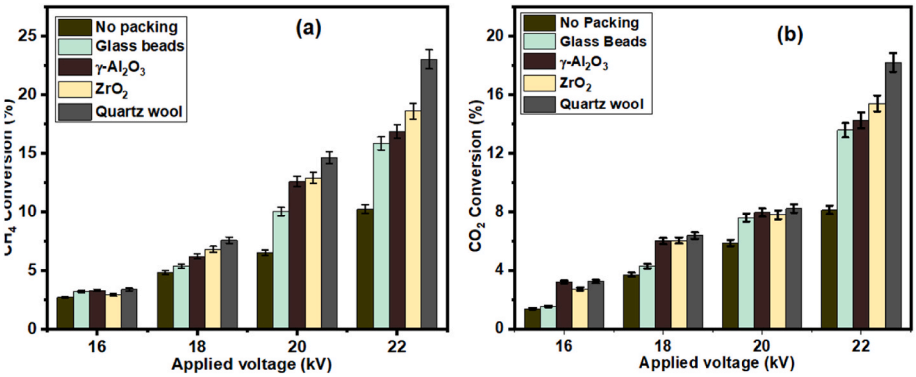

Fig. 4. (a) Represents the conversion of CH_4 (b) Represents the conversion of CO_2 with applied voltage (absence of H_2S).

characteristics and therefore plays a crucial role in the conversion process.

3.3. Effect of the feed gas ratio and packed bed on biogas reforming

Biogas does not have a fixed composition of CH_4 and CO_2. Hence, we analyzed two compositions of gas 1:1 (30 mL min^{-1}: 30 mL min^{-1}) and 2:1 (40 mL min^{-1}:20 mL min^{-1}) CH_4 to CO_2 ratio. The rest was balanced using nitrogen gas (10 mL min^{-1}), keeping the overall flow rate of 70 mL min^{-1}. The conversion of CH_4 and CO_2 and syngas ratio (CO/H_2) was observed to be most significantly influenced by biogas composition. Higher CH_4 and CO_2 conversion were achieved with a 1:1 ratio, possibly less conversion was obtained due to the higher concentration of CH_4 in the feed gas of 2:1. Henceforth, we fixed this ratio (1:1) for further reactions in the experiment. Next, we performed a reaction with two different packed bed conditions, half and fully packed the discharge zone with glass beads. Here, better CH_4 and CO_2 conversions were observed with fully packed DBD, probably due to the more intense electric field between the beads and bead and quartz wall. The results are depicted in Fig. 3. Therefore, the biogas reforming reaction was performed with a 1:1 ratio, and the discharge zone fully packed with a dielectric material to improve the reaction efficiency.

3.4. Effect of applied voltage on reactant conversion, selectivity, and product yield in biogas reforming

The conversion of reactant molecules increases as applied voltage increases. As seen from the data presented in Fig. 4, packed bed DBD

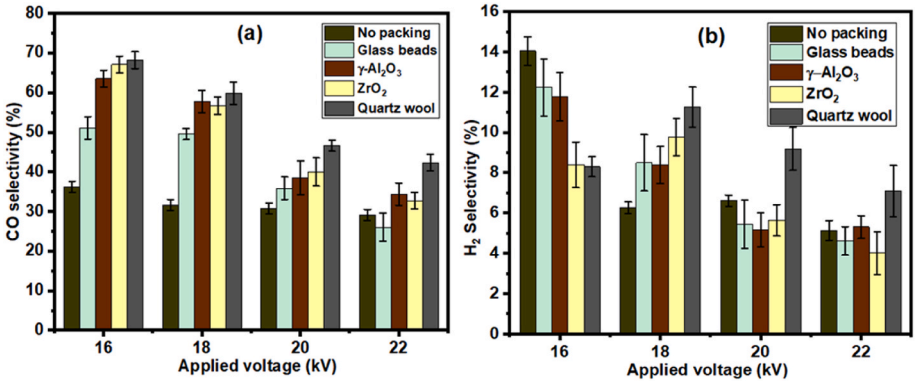

Fig. 5. (a) Represents the CO selectivity with applied voltage. (b) Represents the H_2 selectivity with applied voltage at a fixed flow rate of 70 mL min^{-1} absence of H_2S with a fixed frequency of 50 Hz.

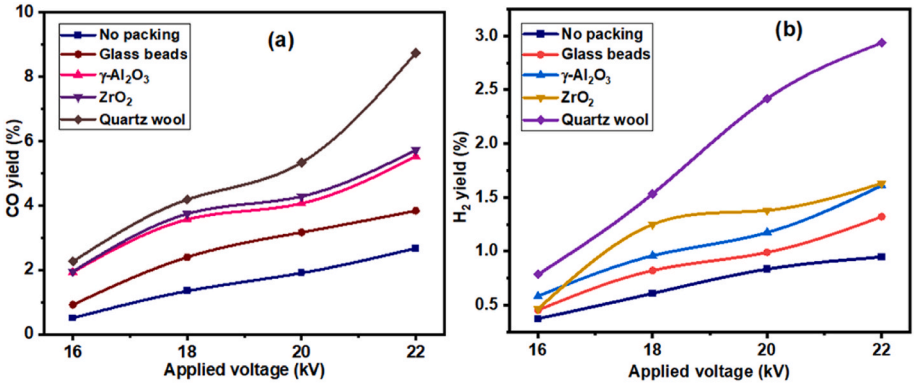

Fig. 6. (a) Represents the CO yield (b) Represents the H_2 yield with applied (absence of H_2S).

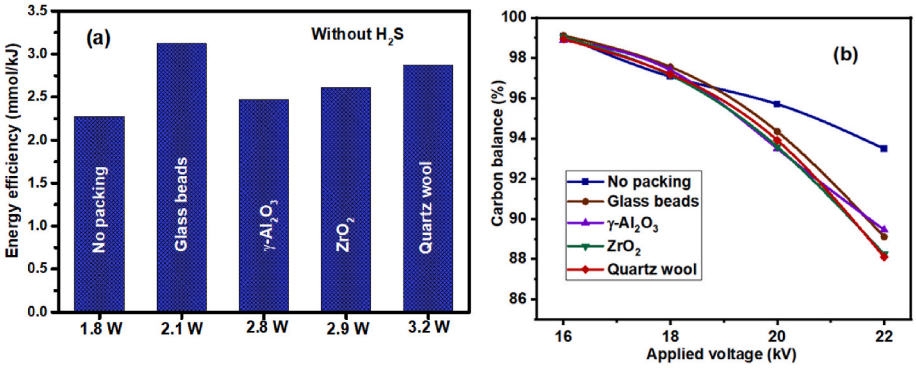

Fig. 7. (a) Represents the energy efficiency with the highest power. (b) Represents the carbon balance with applied voltage (absence of H_2S).

provided higher conversion than no packed DBD throughout the range of applied voltage. The packaging in the DBD reactor enhances discharge strength and plasma parameters in the discharge zone. Hence, packed bed DBD provides more conversion than no packing DBD. Among all packed materials studied, DBD packed with quartz wool resulted in more conversion of CH_4 and CO_2. In the presence of quartz wool, a higher number of current pulses are developed in the discharge zone, improving the residence time effect. Because of this, there is an increased possibility of more CH_4 and CO_2 molecules being present in the discharge zone and converted into CO and H_2. Some studies reported that higher hydrocarbons also form in this reaction. Debjyoti et al. (2020) reported that this reaction also formed C_2, C_3, and C_4 hydrocarbons [34,39]. But in our study, we didn't observe any other higher hydrocarbons, probably due to analytical facilities limitations. The reaction mechanism of CH_4 dissociation and CO_2 dissociation are provided in the supplementary information Sec.4.

The distribution of products is mainly influenced by the feed gas composition and packed bed effect. The major products formed from this reaction are CO and H_2. Higher selectivity of CO and H_2 was achieved with a packed DBD reactor compared with an empty DBD reactor, as shown in Fig. 5. One interesting observation is that as the applied voltage increased, the selectivity of both CO and H_2 decreased in all cases. This may be due to the possibility of the Boudouard reaction in the discharge zone [40]. Coke formation also takes place during the reaction in the discharge zone, and it is deposited on the inner walls of the quartz tube and the surface of the inner electrode. The poor selectivity of H_2 in this reaction is due to the less probable reverse water gas shift reaction, and higher hydrocarbons also may form. However, these higher hydrocarbons were not detected in our GC.

From Eqs. (5) and (6), we have calculated CO and H_2 yield without H_2S. CO and H_2 yields increased with applied voltage in all the cases, as shown in Fig. 6. The packed DBD generated more CO and H_2 yield compared to the no-packing DBD reactor. Quartz wool packed DBD generated the highest CO and H_2 yield among all packed materials. The CO and H_2 yield follow the order: quartz wool > ZrO_2 > γ-Al_2O_3 > glass beads > no packing.

3.5. Energy efficiency and carbon balance of packed materials towards biogas reforming

The energy efficiency of a plasma reactor for gas conversion was calculated using the number of moles of gas converted per unit of plasma power (Eq. (9)). The energy efficiency was estimated at the maximum discharge power in an empty plasma reactor and DBD packed with dielectric materials, as shown in Fig. 7a. The maximum energy efficiency obtained with glass beads is ~3.12 mmol/kJ. The packed DBD showed more energy efficiency in all the cases compared to no packing. Even though the energy efficiency does not vary much when different dielectric materials are used. Energy efficiency follows the order: glass beads > quartz wool > ZrO_2 > γ-Al_2O_3 > no packing. Carbon balance as a function of the applied voltage is presented in Fig. 7b. However, the lowest carbon balance of ~88% was observed with the quartz wool packed DBD at the highest applied voltage. At the same applied voltage, the empty reactor showed a higher carbon balance of ~94%. The carbon balance decreased as the applied voltage increased in all the cases. The main reason was the formation of solid carbon on the surface of the inner electrode and walls of the quartz tube during the biogas reforming reaction.

3.6. Influence of H_2S on biogas reforming

3.6.1. H_2S effect

After performing a biogas reforming experiment without H_2S, similar experiments were carried out in the presence of H_2S to test the influence

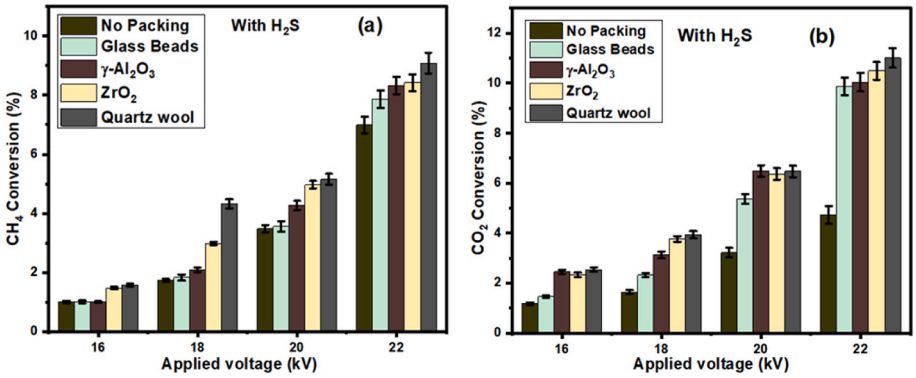

Fig. 8. (a) Effect of H_2S on CH_4 conversion (b) Effect of H_2S on CO_2 conversion with applied voltage.

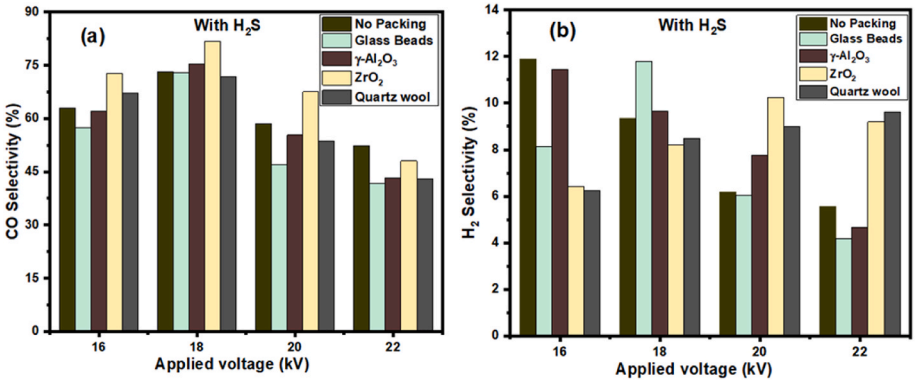

Fig. 9. (a) Effect of H_2S on CO selectivity (b) Effect of H_2S on H_2 selectivity with applied voltage.

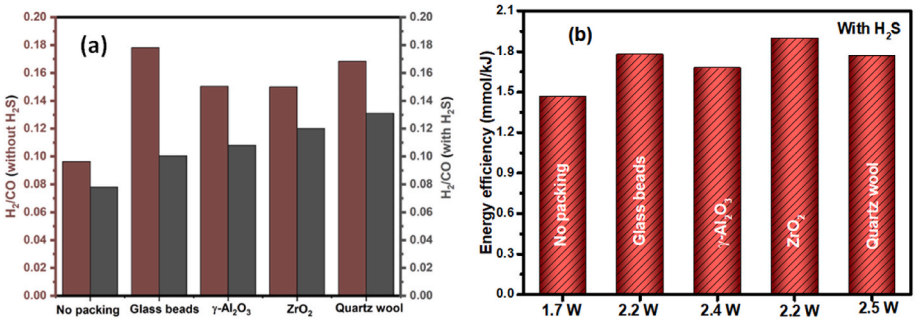

Fig. 10. (a) A gas ratio of H_2/CO for dielectric materials at an applied voltage of 22 kV with the absence and presence of H_2S. (b) Represents the energy efficiency with the highest power with H_2S.

of H_2S on the biogas reforming reaction under packed with dielectric materials in the DBD reactor. CH_4 and CO_2 conversion data are presented in Fig. 8. From Fig. 8a, it can be observed that CH_4 conversion drastically decreased from 23% (without H_2S) to 9% (with H_2S) with quartz wool packed DBD, and Fig. 8b shows that the CO_2 conversion drastically decreased from 18% to 11% at 22 kV. A similar trend was observed. The results show that the reaction's gas composition has poisoning effect prominently. Based on this conversion, we may consider that the influence of H_2S is more on CH_4 than CO_2.

3.6.2. *Influence of H_2S on selectivity to syngas*

The presence of H_2S in the reaction mixture influences the H_2 and CO selectivity. We found that the H_2S had minimal effect on selectivity in our experiments. H_2S has a more significant influence on conversion and syngas gas ratio than selectivity. Fig. 9 depicts CO and H_2 selectivity with applied voltage.

3.7. *Syngas ratio and energy efficiency of packed bed DBD for biogas reforming*

As shown in Fig. 10a, the product gas H_2/CO ratio in the packed DBD was always greater than no packing DBD both in the absence of H_2S and the presence of H_2S. The maximum syngas ratio of 0.18 was achieved with glass beads packed DBD in the absence of H_2S, as follows: glass beads > quartz wool > ZrO_2 > γ-Al_2O_3 > no packing. The syngas ratio is not very much different for different dielectric materials. After the addition of H_2S in the reaction mixture, the syngas ratio decreased in all the cases due to the poison effect. Carbon formed during the reaction, a less possible reverse water-gas shift reaction (Eq. (10)) and reverse Boudouard reaction (Eq. (11)) may play a small role in the decreasing syngas ratio. The presence of H_2S affected the conversion of CH_4 and CO_2 during the reaction in both packed and unpacked DBD. Because of this, the formation of H_2 and CO are less; hence the syngas ratio

decreased relative to the biogas reforming reaction without H_2S. The energy efficiency is also affected when H_2S is added to the reaction mixture, as shown in Fig. 10b. Because of the poison effect, in all the experiments, energy efficiency decreased compared to the reactions performed without H_2S, as shown in Fig. 7a. From Fig. 10b packed DBD shows better energy efficiency than no pack DBD. The order of energy efficiency: ZrO_2 > quartz wool > glass beads > γ-Al_2O_3 > no packing.

$$CO_2 + H_2 \rightarrow CO + H_2O \quad (10)$$

$$CO_2 + C \rightarrow 2CO \quad (11)$$

4. Conclusions

This study showed that non-thermal plasma is a useful tool for converting biogas into syngas under ambient conditions. The conversion of CH_4 and CO_2 is dependent on the discharge power with voltage variations. The influence of feed gas ratio and packed bed conditions on the conversion of CH_4 and CO_2 was studied. While increasing the applied voltage, the total consumption of electric energy also rises, stimulating the production of more high-energy electrons, ions, and free radicals, resulting in a noticeable increase in the biogas conversion rate. The dielectric materials packed DBD improved the reaction performance compared to no packed DBD. The results indicate that reaction performance mainly depends on the dielectric constant and shape of the materials. A DBD reactor packed with quartz wool has the best reaction performance. The influence of H_2S on reaction performance was investigated. It was observed that even with the addition of 0.054 mol% of H_2S, the CH_4 and CO_2 conversions were significantly reduced. Furthermore, due to its poisonous nature, H_2S impacts the syngas ratio and energy efficiency. As a result of the findings of this study, it is possible to conclude that ignoring the presence of H_2S while investigating biogas reforming is not an accurate assumption.

Data availability

Data will be made available on request.

Acknowledgments

M. U. Rao would like to thank the University of Grants Commission, India for providing Junior Research Fellowship. We acknowledge Indian Institute of Technology Hyderabad for the Research facilities.

Appendix A. Supplementary data

Supplementary data to this article can be found online at https://doi.org/10.1016/j.biombioe.2023.106781.

References

[1] M.-S. Fan, A.Z. Abdullah, S. Bhatia, Catalytic technology for carbon dioxide reforming of methane to synthesis gas, ChemCatChem 1 (2009) 192–208, https://doi.org/10.1002/cctc.200900025.
[2] N. Abatzoglou, S. Boivin, A review of biogas purification processes, Biofuels Bioprod. Biorefining. 3 (2009) 42–71, https://doi.org/10.1002/bbb.117.
[3] M. Zhumabek, G. Xanthopoulou, S.A. Tungatarova, T.S. Baizhumanova, G. Vekinis, D.Y. Murzin, Biogas reforming over Al-Co catalyst prepared by solution combustion synthesis method, Catalysts 11 (2021) 274, https://doi.org/10.3390/catal11020274.
[4] S.A. Chattanathan, S. Adhikari, S. Taylor, Conversion of carbon dioxide and methane in biomass synthesis gas for liquid fuels production, Int. J. Hydrogen Energy 37 (2012) 18031–18039, https://doi.org/10.1016/j.ijhydene.2012.08.108.
[5] H. Özdemir, M.A.F. Öksüzömer, M.A. Gürkaynak, Effect of the calcination temperature on Ni/MgAl2O4 catalyst structure and catalytic properties for partial oxidation of methane, Fuel 116 (2014) 63–70, https://doi.org/10.1016/j.fuel.2013.07.095.
[6] B. Hernandez, M. Martin, Optimization for biogas to chemicals via tri-reforming. Analysis of Fischer-Tropsch fuels from biogas, Energy Convers. Manag. 174 (2018) 998–1013, https://doi.org/10.1016/j.enconman.2018.08.074.
[7] R. Hakawati, B. Smyth, H. Daly, G. McCullough, D. Rooney, Is the fischer-tropsch conversion of biogas-derived syngas to liquid fuels feasible at atmospheric pressure? Energies 12 (2019) 1031, https://doi.org/10.3390/en12061031.
[8] J.-L. Liu, H.-W. Park, W.-J. Chung, W.-S. Ahn, D.-W. Park, Simulated biogas oxidative reforming in AC-pulsed gliding arc discharge, Chem. Eng. J. 285 (2016) 243–251, https://doi.org/10.1016/j.cej.2015.09.100.
[9] B. Ashford, X. Tu, Non-thermal plasma technology for the conversion of CO2, Curr. Opin. Green Sustain. Chem. 3 (2017) 45–49, https://doi.org/10.1016/j.cogsc.2016.12.001.
[10] S. Liu, D. Mei, L. Wang, X. Tu, Steam reforming of toluene as biomass tar model compound in a gliding arc discharge reactor, Chem. Eng. J. 307 (2017) 793–802, https://doi.org/10.1016/j.cej.2016.08.005.
[11] H. Zhang, X. Li, F. Zhu, K. Cen, C. Du, X. Tu, Plasma assisted dry reforming of methanol for clean syngas production and high-efficiency CO2 conversion, Chem. Eng. J. 310 (2017) 114–119, https://doi.org/10.1016/j.cej.2016.10.104.
[12] X. Zhao, B. Joseph, J. Kuhn, S. Ozcan, Biogas reforming to syngas: a review, iScience 23 (2020), 101082, https://doi.org/10.1016/j.isci.2020.101082.
[13] Y. Zeng, X. Zhu, D. Mei, B. Ashford, X. Tu, Plasma-catalytic dry reforming of methane over γ-Al2O3 supported metal catalysts, Catal. Today 256 (2015) 80–87, https://doi.org/10.1016/j.cattod.2015.02.007.
[14] Y.X. Zeng, L. Wang, C.F. Wu, J.Q. Wang, B.X. Shen, X. Tu, Low temperature reforming of biogas over K-, Mg- and Ce-promoted Ni/Al2O3 catalysts for the production of hydrogen rich syngas: understanding the plasma-catalytic synergy, Appl. Catal. B Environ. 224 (2018) 469–478, https://doi.org/10.1016/j.apcatb.2017.10.017.
[15] G. Chen, X. Tu, G. Homm, A. Weidenkaff, Plasma pyrolysis for a sustainable hydrogen economy, Nat. Rev. Mater. 7 (2022) 333–334, https://doi.org/10.1038/s41578-022-00439-8.
[16] X. Tu, J.C. Whitehead, Plasma-catalytic dry reforming of methane in an atmospheric dielectric barrier discharge: understanding the synergistic effect at low temperature, Appl. Catal. B Environ. 125 (2012) 439–448, https://doi.org/10.1016/j.apcatb.2012.06.006.
[17] S.S. Tabaie, D. Iraji, R. Amrollahi, Measurement of electron temperature and density of atmospheric plasma needle, Vacuum 182 (2020), 109761, https://doi.org/10.1016/j.vacuum.2020.109761.
[18] A. George, B. Shen, M. Craven, Y. Wang, D. Kang, C. Wu, X. Tu, A Review of Non-thermal Plasma Technology: a novel solution for CO2 conversion and utilization, Renew. Sustain. Energy Rev. 135 (2021), 109702, https://doi.org/10.1016/j.rser.2020.109702.
[19] D. Mei, G. Duan, J. Fu, S. Liu, R. Zhou, R. Zhou, Z. Fang, P.J. Cullen, K. (Ken) Ostrikov, CO2 reforming of CH4 in single and double dielectric barrier discharge reactors: comparison of discharge characteristics and product distribution, J. CO2 Util. 53 (2021), 101703, https://doi.org/10.1016/j.jcou.2021.101703.
[20] Y. Diao, X. Zhang, Y. Liu, B. Chen, G. Wu, C. Shi, Plasma-assisted dry reforming of methane over Mo2C-Ni/Al2O3 catalysts: effects of β-Mo2C promoter, Appl. Catal. B Environ. 301 (2022), 120779, https://doi.org/10.1016/j.apcatb.2021.120779.
[21] J. Martin-del-Campo, M. Uceda, S. Coulombe, J. Kopyscinski, Plasma-catalytic dry reforming of methane over Ni-supported catalysts in a rotating gliding arc – spouted bed reactor, J. CO2 Util. 46 (2021), 101474, https://doi.org/10.1016/j.jcou.2021.101474.
[22] D. Mei, B. Ashford, Y.-L. He, X. Tu, Plasma-catalytic reforming of biogas over supported Ni catalysts in a dielectric barrier discharge reactor: effect of catalyst supports, Plasma Process. Polym. 14 (2017), 1600076, https://doi.org/10.1002/ppap.201600076.
[23] A. Wang, J.H. Harrhy, S. Meng, P. He, L. Liu, H. Song, Non-thermal plasma-catalytic conversion of biogas to liquid chemicals with low coke formation, Energy Convers. Manag. 191 (2019) 93–101, https://doi.org/10.1016/j.enconman.2019.04.026.
[24] X. Zheng, S. Tan, L. Dong, S. Li, H. Chen, Silica-coated LaNiO3 nanoparticles for non-thermal plasma assisted dry reforming of methane: experimental and kinetic studies, Chem. Eng. J. 265 (2015) 147–156, https://doi.org/10.1016/j.cej.2014.12.035.
[25] D. Ray, P. Chawdhury, Ch Subrahmanyam, 1. A facile method to decompose CO2 using a g-C3N4-assisted DBD plasma reactor, Environ. Res. 183 (2020), 109286, https://doi.org/10.1016/j.envres.2020.109286.
[26] M.-W. Li, Y.-L. Tian, G.-H. Xu, Characteristics of carbon dioxide reforming of methane via alternating current (AC) corona plasma reactions, Energy Fuel. 21 (2007) 2335–2339, https://doi.org/10.1021/ef070146k.
[27] A. Aziznia, H.R. Bozorgzadeh, N. Seyed-Matin, M. Baghalha, A. Mohamadalizadeh, Comparison of dry reforming of methane in low temperature hybrid plasma-catalytic corona with thermal catalytic reactor over Ni/γ-Al2O3, J. Nat. Gas Chem. 21 (2012) 466–475, https://doi.org/10.1016/S1003-9953(11)60392-7.
[28] D. Li, X. Li, M. Bai, X. Tao, S. Shang, X. Dai, Y. Yin, CO2 reforming of CH4 by atmospheric pressure glow discharge plasma: a high conversion ability, Int. J. Hydrogen Energy 34 (2009) 308–313, https://doi.org/10.1016/j.ijhydene.2008.10.053.
[29] J.-Y. Wang, G.-G. Xia, A. Huang, S.L. Suib, Y. Hayashi, H. Matsumoto, CO2 decomposition using glow discharge plasmas, J. Catal. 185 (1999) 152–159, https://doi.org/10.1006/jcat.1999.2499.
[30] Z. Bo, J. Yan, X. Li, Y. Chi, K. Cen, Plasma assisted dry methane reforming using gliding arc gas discharge: effect of feed gases proportion, Int. J. Hydrogen Energy 33 (2008) 5545–5553, https://doi.org/10.1016/j.ijhydene.2008.05.101.
[31] X. Tu, J.C. Whitehead, Plasma dry reforming of methane in an atmospheric pressure AC gliding arc discharge: Co-generation of syngas and carbon

nanomaterials, Int. J. Hydrogen Energy 39 (2014) 9658–9669, https://doi.org/10.1016/j.ijhydene.2014.04.073.
[32] Q. Wang, B. Spasova, V. Hessel, G. Kolb, Methane reforming in a small-scaled plasma reactor – industrial application of a plasma process from the viewpoint of the environmental profile, Chem. Eng. J. 262 (2015) 766–774, https://doi.org/10.1016/j.cej.2014.09.091.
[33] U. Kogelschatz, Dielectric-barrier discharges: their history, discharge physics, and industrial applications, Plasma Chem. Plasma Process. 23 (2003) 1–46, https://doi.org/10.1023/A:1022470901385.
[34] Y. Zeng, G. Chen, Q. Bai, L. Wang, R. Wu, X. Tu, Biogas reforming for hydrogen-rich syngas production over a Ni–K/Al2O3 catalyst using a temperature-controlled plasma reactor, Int. J. Hydrogen Energy (2022), https://doi.org/10.1016/j.ijhydene.2022.06.135. S0360319922027689.
[35] Y.J.O. Asencios, J.D.A. Bellido, E.M. Assaf, Synthesis of NiO–MgO–ZrO2 catalysts and their performance in reforming of model biogas, Appl. Catal. Gen. 397 (2011) 138–144, https://doi.org/10.1016/j.apcata.2011.02.023.
[36] J. Xu, W. Zhou, Z. Li, J. Wang, J. Ma, Biogas reforming for hydrogen production over nickel and cobalt bimetallic catalysts, Int. J. Hydrogen Energy 34 (2009) 6646–6654, https://doi.org/10.1016/j.ijhydene.2009.06.038.
[37] D. Mei, X. Zhu, Y.-L. He, J.D. Yan, X. Tu, Plasma-assisted conversion of CO2 in a dielectric barrier discharge reactor: understanding the effect of packing materials, Plasma Sources Sci. Technol. 24 (2014), 015011.
[38] A.H. Khoja, M. Tahir, N.A.S. Amin, Dry reforming of methane using different dielectric materials and DBD plasma reactor configurations, Energy Convers. Manag. 144 (2017) 262–274, https://doi.org/10.1016/j.enconman.2017.04.057.
[39] D. Ray, P. Chawdhury, C. Subrahmanyam, Promising utilization of CO2 for syngas production over Mg2+- and Ce2+-promoted Ni/γ-Al2O3 assisted by non-thermal plasma, ACS Omega 5 (2020) 14040–14050, https://doi.org/10.1021/acsomega.0c01442.
[40] O.A. Bereketidou, M.A. Goula, Biogas reforming for syngas production over nickel supported on ceria–alumina catalysts, Catal. Today 195 (2012) 93–100, https://doi.org/10.1016/j.cattod.2012.07.006.